The low-lying electronic states of SiO

Charles W. Bauschlicher, Jr.*†

NASA Ames Research Center, Moffett Field, CA 94035

Abstract

The singlet states of SiO that correlate with ground state atoms have been studied. The

computed spectroscopic constants are in good agreement with experiment. The lifetime of

the E state has been calculated to be 10.9 ns; this is larger than the results of previous

computations and is in excellent agreement with the experimental value of 10.5 ± 1.1 ns. The

lifetime of the A state is about three times larger than found in experiment. We suggest

that absorption from the X state to the $(2)^{1}\Pi$ state is responsible for the unidentified lines

in the experiment of Hormes et al.

Keywords: electronic transition

* Mail Stop 230-3, Entry Systems and Technology Division

1

I. INTRODUCTION

Meteor entry produces emission that can be observed on earth. This arises from the air heated by the bow shock and from the products of the reaction of the hot air and the ablation gases from the meteor. Stony meteors contain a large fraction of silicate rocks that yield Si atoms as ablation products, that can react with oxygen atoms in the wake. This reaction yields SiO in electronically excited states that can emit and contribute to the observed meteor emission. High fidelity modeling of such emission requires accurate electronic transition intensities for low-lying states.

There have been numerous studies of SiO, both experimental¹⁻⁶ and theoretical⁷⁻¹⁰. While much is know about SiO emission, the lifetime of the $A^1\Pi$ state is still in question. An experimental value³ of 9.6 ± 1 ns has been reported. Computed⁷⁻¹⁰ lifetimes for this state have varied for 49.5 to 12.5 ns. For the E state the computed lifetimes⁸⁻¹⁰ are about 70% of the measured value⁴. While the agreement between theory and experiment E state is better than for the A state, it is still worthwhile to reinvestigate this transition as well. Given that this is expected to be an observed emission from meteor entry, it is important to correctly establish the A-X and E-X emission intensity. We have therefore studied the singlet states of SiO that correlate with ground state atoms.

II. METHODS

We consider the six singlet states arising from ground state Si $(^{3}P_{g})$ and O $(^{3}P_{g})$ atoms. The two $^{1}\Sigma^{+}$, one $^{1}\Sigma^{-}$, two $^{1}\Pi$, and one $^{1}\Delta$ state are treated using the dynamically weighed 11 state-averaged complete active space self-consistent-field (DW-SA-CASSCF) approach. The Si 1s, 2s, and 2p orbitals and the O 1s and 2s orbitals are treated as inactive. The oxygen 2p and 2p' and silicon 3s and 3p orbitals are in the active space. More extensive correlation is included using the internally contracted multireference configuration interaction (IC-MRCI) approach 12 . The CASSCF configurations are included in the reference space and the oxygen 2s orbital is also correlated in the IC-MRCI calculations. The augmented correlation consistent quintuple zeta (aug-cc-pV5Z) basis $^{13-15}$ is used. The calculations are preformed using MOL-

 $PRO^{12,16-18}$.

In the typical approach the phase of the transition moments is undefined. We avoid this uncertainty following the suggestion of Schwenke¹⁹. We pick one r value as reference and perform a standard calculation. We perform the CASSCF calculation for the adjacent point and compute the diabatic orbitals. This makes the orbitals at the second point as similar as possible to those at the first, or reference point. We Schmidt orthogonalize the reference orbitals at the displaced geometry and compute the overlap between the two sets to confirm that the overlap is larger than 0.5 for analogous pairs of orbitals. We note that while we use diabetic orbitals, we are not performing diabetic calculations. After performing the IC-MRCI, we compute the overlap between the CI vectors for these two points. Since the orbitals are similar and have the same phase, the overlap of the CI vectors allows the phase of the transition moments to be made consistent. We should note that one cannot use a single point as reference for the entire curve since the orbitals change too much for points that differ significantly in r value. So we proceed stepwise and use the previous r value as reference.

The Einstein A values and lifetimes are computed in the standard manner using the computed potentials and computed transition moments. When the experimental T_0 is known from experiment, the computed potentials are shifted to match experiment.

III. RESULTS AND DISCUSSION

The IC-MRCI potentials are plotted in Fig. 1 and the computed spectroscopic constants are summarized in Table I along the experimental results. The agreement of the computed and experimental spectroscopic constants is quite good. The D_0 values differ by 0.01 eV, the r_e values differ by a maximum of 0.014 Å, the T_e values differ by a maximum of 430 cm⁻¹, and the ω_e values by a maximum of 12 cm⁻¹. The potentials for the C and D states are extremely similar. An inspection of wave functions shows that the occupations have nearly the same weight, just differing in the coupling of the angular moment. While there are no experimental results for the $(2)^1\Pi$ state, we can expect similar accuracy for this state. Our potentials do not

have barriers for the E and $(2)^{1}\Pi$ states as found by Chattopadhyaya et al.¹⁰ and is probably a result of using the CASSCF with a large active space and addition of extensive correlation in the IC-MRCI approach.

The moments as computed, with no changes in the phase, are plotted in Figs. 2-5; clearly the procedure of using diabetic orbitals and computing the overlap of the CI vectors simplifies calculation of the transition moments. We note that the $(2)^1\Pi - A^1\Pi$ transition moment is near zero in the Franck-Condon region, which is not too surprising as the two states differ by two orbitals; the A occupation is ... $6\sigma^27\sigma^11\pi^42\pi^43\pi^1$ while the $(2)^2\Pi$ state occupation is ... $6\sigma^27\sigma^28\sigma^11\pi^42\pi^3$. The $C - {}^1\Pi$ and $D - {}^1\Pi$ moments are very similar, which is consistent with the C and D states having similar compositions, differing only in the coupling of the angular momentum.

The computed lifetimes for the few lowest vibrational levels of the excited states are summarized in Table II. The two lowest excited states, the $C^1\Sigma^-$ and $D^1\Delta$ cannot decay by a dipole allowed transition. The $A^1\Pi$ state is the first excited state that has dipole allowed transitions. It can decay to all three of the lower states, however, the small energy difference between the A, C, and D states means that the A lifetime is essentially completely determined by the A-X transition. Because of the difference in r_e values for the X and A states, there are several strong transitions for each ν' level, for example the Franck-Condon values for $\nu'=0$ are 0.116, 0.254, 0.275, 0.195, and 0.101 for the ν'' levels, 0, 1, 2, 3, and 4, respectively. Our computed lifetime for $\nu'=0$ using only theory is 29.3 ns, but is increased to 30.3 ns if the experimental separations. These values are in excellent agreement with the value of 31.6 ns computed by Oddershede and Elander using their computed moment and experimental potential. Using their computed potential yielded 49.5 ns. This is also in very good agreement with the 28.9 ns reported by Chattopadhyaya et al. 10 Our value is significantly larger than the computed values of Langhoff and Arnold⁸ (16.6 ns) and of Drira et al.⁹ (13.6 ns) and the experimental value of Smith and Liszt³ (9.6 \pm 1.0 ns).

The difference between our lifetime and those of Langhoff and Arnold and of Drira et al. is hard to reconcile. Langhoff and Arnold reports an $|R_e|^2$ value of slightly more than 1. a.u. at r=3.0 bohr, which is similar to our value of 1.08 a.u. at the same bond length using the same definition for $|R_e|^2$. While the degeneracy of the $A^1\Pi$

state results in twice the emission compared with a nondegenerate state, both the components decay at the same rate, which is the same as for a nondegenerate state. Thus the transition moment used the calculation of the lifetime needs to be a factor of two smaller than that deduced from the emission. Given the very similar $|R_e|^2$ values for our work and that of Langhoff and Arnold, but lifetimes that differ by a factor of two, we suspect they have an extra factor of two in their lifetime calculation and their value should be 33.2 ns, which is very similar to our value. It is a bit more difficult to compare with the work of Drira et al. as their Figs. 2 and 3 have some of the data switched between the A and E states. They appear to show an $|R_e|^2$ of about 0.8 a.u. in their Fig. 2, but they report a shorter lifetime than Langhoff and Arnold. We cannot explain their shorter lifetime given the smaller $|R_e|^2$.

The large difference between our calculations and experiment is unexpected as we have used very accurate methods. Park and Arnold⁶ deduced an $|R_e|^2$ curve from their experiments that was very similar to that reported by Langhoff and Arnold⁸ (and hence also similar to our values); this would appear to support the computed results and hence the longer lifetime. It is possible that there is no real disagreement on the emission, but rather the lifetime measured by Smith and Liszt is reduced by curve crossing to one of the four known² perturbing states, which is not accounted for in our calculations. Given the difference between theory and experiment, a new experimental study of SiO A state lifetime would seem ideal.

The $E^1\Sigma^+$ state has dipole allowed transitions to the A and X states. The emission to the X is about 4 orders of magnitude larger than to the A state, so the lifetime of the E state is determined by the transitions to the X state. Due to the significant difference in r_e values, the Franck-Condon factors for the v'=0 are 0.001, 0.007, 0.026, 0.062, 0.1094, 0.151, 0.169, 0.158, 0.127, and 0.0874 for v''=0 to 9. Our lifetime for v'=0 of 10.9 ns is larger than the computed values of 6.8 ns by Langhoff and Arnold, 6.68 ns by Drira et al. and 7.4 ns by Chattopadhyaya et al., but in excellent agreement with the experimental lifetime of 10.5 ± 1.1 ns by Elander and Smith⁴. We suspect that our larger basis set and higher levels of correlation treatment are responsible for our improved agreement with experiment.

The at approximately 62000 cm⁻¹ does not appear to have been identified in

experiment, but was previously reported by Chattopadhyaya et al. This state is quite shallow, but supports 9 vibrational levels. It has dipole allowed transitions to all of the lower states, but lifetime is essentially determined by decay to the X state. Our lifetime of 29.7 ns is about twice that of Chattopadhyaya et al. Thus difference between our lifetimes and those of Chattopadhyaya et al. increase from the A to E and on to the $(2)^2\Pi$ state. We attribute the difference to the higher level of theory used in our work. Because of the significant difference in r_e values, the emission from a given v' level is spread out into many v'' levels. To aid in possible identification of this state, we have reported the Einstein A coefficients for emission from the v'=0 and 1 levels of this state to the lower states with A values larger than $1.x10^5$. As shown in Table III most of the large bands are to the X states.

The Franck-Condon factors and energy separations for the absorption from the v''=0 level of the X state to the $(2)^1\Pi$ state are given in Table IV. These values are consistent with the unidentified lines given by Hormes et al.¹ and we suspect that transitions to the $(2)^1\Pi$ are responsible for these lines.

IV. CONCLUSIONS

The singlet states of SiO that correlate with ground state atoms have been studied. The computed spectroscopic constants are in good agreement with experiment. The lifetime of the E state is in excellent agreement with experiment, while that of the A state is about three times that of experiment. Given the accurate treatment used in this work, we suggest that new experimental studies of the A state lifetime are warranted. We also suggest that absorption from the X state to the $(2)^2\Pi$ state are responsible for the unidentified lines in the experiment of Hormes et al.

V. ACKNOWLEDGMENTS

The author would like to acknowledge helpful discussions with David Schwenke.

- $^5\,$ C. Park, J. Spectroc. Radiat. Transfer 20 (1978) 491.
- ⁶ C. Park, J.O. Arnold, J. Spectroc. Radiat. Transfer 19 (1979) 1.
- ⁷ J. Oddershede, N. Elander, J. Chem. Phys. 65 (1976) 3495.
- ⁸ S.R. Langhoff, J.O. Arnold, J. Chem. Phys. 70 (1979) 852.
- ⁹ I. Drira, A. Spielfiedel, S. Edwards, N. Feautrier, J. Spectroc. Radiat. Transfer 60 (1998)
 1.
- ¹⁰ S. Chattopadhyaya, A. Chattopadhyayam K. K. Das, J. Phys. Chem. A 107 (2003) 148.
- ¹¹ M.P. Deskevich, D.J. Nesbitt, H.-J. Werner, J. Chem. Phys. 120 (2004) 7281.
- ¹² H.-J. Werner, P.J. Knowles, J. Chem. Phys. 89 (1988) 5803; P.J. Knowles, H.-J. Werner, Chem. Phys. Lett. 145 (1988) 514.
- ¹³ T. H. Dunning, J. Chem. Phys. 90 (1989)1007-1023.
- ¹⁴ R.A. Kendall, T.H. Dunning, R.J. Harrison, J. Chem. Phys. 96 (1992) 6796-6806.
- ¹⁵ D.E. Woon, T. H. Dunning, J. Chem. Phys., 98 (1993) 1358-71.
- MOLPRO, version 2010.1, a package of ab initio programs, H.-J. Werner, P. J. Knowles, F. R. Manby, M. Schütz, P. Celani, G. Knizia, T. Korona, R. Lindh, A. Mitrushenkov, G. Rauhut, T. B. Adler, R. D. Amos, A. Bernhardsson, A. Berning, D. L. Cooper, M. J. O. Deegan, A. J. Dobbyn, F. Eckert, E. Goll, C. Hampel, A. Hesselmann, G. Hetzer, T. Hrenar, G. Jansen, C. Köppl, Y. Liu, A. W. Lloyd, R. A. Mata, A. J. May, S. J. McNicholas, W. Meyer, M. E. Mura, A. Nicklass, P. Palmieri, K. Pflüger, R. Pitzer, M. Reiher, T. Shiozaki, H. Stoll, A. J. Stone, R. Tarroni, T. Thorsteinsson, M. Wang, A.

[†] Electronic address: Charles.W.Bauschlicher@nasa.gov

 $^{^{1}\,}$ J. Hormes, M. Sauer, R. Scullman, J. Mol. Spectroc. 98 (1983) 1.

² R.W. Field, A. Lagerqvist, I Renhorn, Phys. Scrip. 14 (1976) 298.

³ W.H. Smith, H.S. Liszt, J. Quant. Spectroc. Radiat. Transfer 12 (1972) 505.

 $^{^4\,}$ N. Elander W.H. Smith, Astro. Phys. J. 184 (1973) 311.

Wolf, see http://www.molpro.net.

- $^{17}\,$ R. Lindh, U. Ryu, B. Liu, J. Chem. Phys. 95 (1991) 5889.
- $^{18}\,$ P. J. Knowles, H.-J. Werner, Chem. Phys. Lett. 115 (1985) 259.
- ¹⁹ D.W. Schwenke, personal communication.
- ²⁰ K.P. Huber, G, Herzberg, 1979 "Molecular Spectra and Molecular Structure: IV. Constants of Diatomic Molecules," Van Nostrand Reinhold Company.

TABLE I: Summary of spectroscopic constants.

State	$T_e(\text{cm}^{-1})$		$r_e(ext{Å})$		$\omega_e(\mathrm{cm}^{-1})$		$\omega_e X_e (\mathrm{cm}^{-1})$	
	IC-MRCI	Exp^a	IC-MRCI	Exp	IC-MRCI	Exp	IC-MRCI	Exp
$(2)^1\Pi$	62 304		1.728		610.9		11.24	
$\mathrm{E}^1\Sigma^+$	52 788	52 861	1.741	1.740	673.9	675.5	4.60	4.204
$\mathrm{A}^1\Pi$	43 264	42 835	1.634	1.620	840.8	852.8	6.17	6.43
$\mathrm{D}^1\Delta$	38 641	38 823	1.740	1.729	737.5	730	4.94	3.9
$\mathrm{C}^1\Sigma^-$	38 515	38 624	1.739	1.727	743.3	740	4.96	4.27
$X^1\Sigma^+$	8.25^{b}	8.26	1.517	1.510	1232.3	1241.6	5.56	5.966

 $[^]a$ Huber and Herzberg, Ref. 20

TABLE II: Summary of lifetimes, in ns, for the excited singlet states of SiO.

Level	State					
u'	A		E	·	$(2)^{1}\Pi$	
	Exp^a	Theor	Exp	Theor	Theor	
0	30.3	29.3	10.9	11.0	29.7	
1	30.4	29.5	11.5	11.6	32.2	
2	30.6	29.6	12.2	12.2	34.9	
3	30.7	29.8	12.8	12.9	37.9	
4	30.9	30.0	13.5	13.6	41.2	

^a Indicates that the potentials have been shifted to reproduce the experimental T_0 values.

^b The D_0 in eV.

TABLE III: Computed Franck-Condon (FC) factors, energy separations (ΔE , in cm⁻¹) and Einstein A values larger than $1.x10^5$ for emission from the v'=0 and 1 levels of the $(2)^1\Pi$ to the lower states.

v' v''	FC	$\Delta \mathrm{E}$	A	v' v''	FC	$\Delta \mathrm{E}$	A
$(2)^1\Pi - X$							
0 1	0.014	60 771	0.531E + 06	1 2	0.099	60 150	0.373E + 07
0 2	0.043	59 561	0.162E + 07	1 3	0.121	58 952	0.453E + 07
0 3	0.088	58 364	0.323E+07	1 4	0.090	57 768	0.330E+07
0 4	0.133	57 180	0.476E + 07	1 5	0.033	56 597	0.118E+07
0 5	0.161	56 008	0.553E + 07	1 7	0.016	54 289	0.500E + 06
0 6	0.162	54 848	0.530E + 07	1 8	0.061	53 151	0.182E+07
0 7	0.139	53 700	0.431E + 07	1 9	0.102	52 025	0.286E+07
0 8	0.105	52 563	0.304E+07	1 10	0.118	50 909	0.308E+07
0 9	0.070	51 436	0.189E + 07	1 11	0.107	49 805	0.259E+07
0 10	0.042	50 321	0.105E+07	1 12	0.081	48 711	0.181E+07
0 11	0.023	49 216	0.525E + 06	1 13	0.053	47 629	0.109E+07
0 12	0.011	48 123	0.239E + 06	1 14	0.031	$46\ 558$	0.584E + 06
1 0	0.011	62 581	0.382E + 06	1 15	0.016	45 498	0.279E + 06
1 1	0.048	61 360	0.178E + 07	1 16	0.008	44 449	0.121E+06
	($2)^{1}\Pi - C$			(2)	$\Pi - D$	
0 0	0.989	23 721	0.580E + 06	0 0	0.989	$23\ 598$	0.707E + 06
1 1	0.976	$23\ 577$	0.523E + 06				

TABLE IV: Computed Franck-Condon (FC) factors and energy separations (in cm⁻¹) for the $(2)^1\Pi - X^1\Sigma^+$ absorption from v''=0.

v'	FC	$\Delta \mathrm{E}$
0	0.002	61 992
1	0.011	62 581
2	0.026	63 147
3	0.047	63 693
4	0.067	64 218
5	0.084	64 725
6	0.094	65 214
7	0.097	65 687
8	0.094	66 144

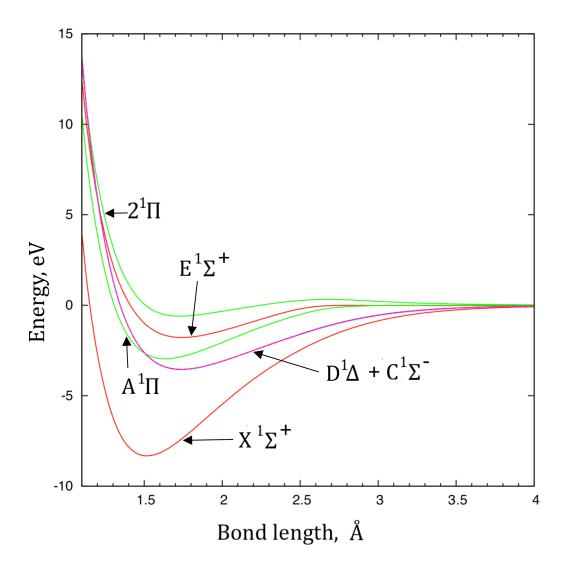


FIG. 1: The computed MRCI potential curves.

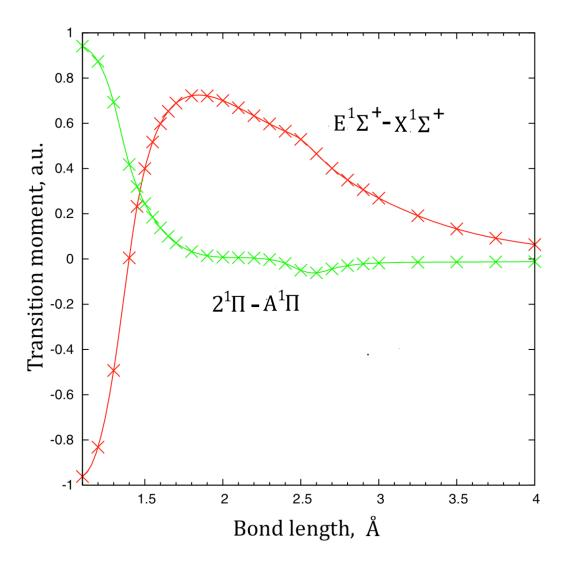


FIG. 2: The computed transition moments for the $E^1\Sigma^+ - X^1\Sigma^+$ and $2^1\Pi - A^1\Pi$ transitions.

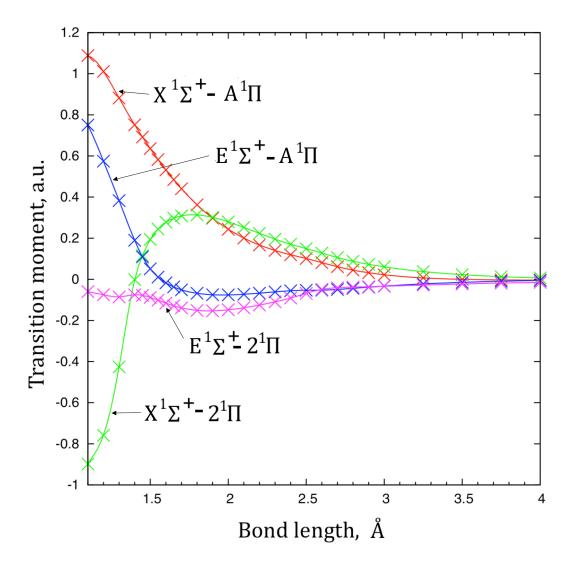


FIG. 3: The computed transition moments for the $^1\Sigma^+$ – $^1\Pi$ transitions.

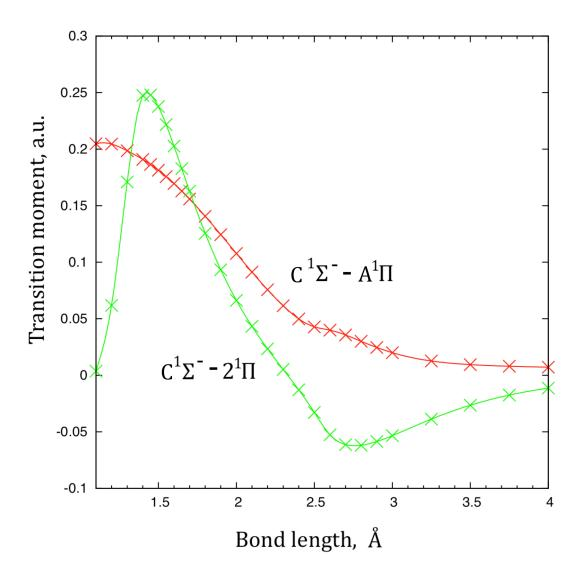


FIG. 4: The computed transition moments for the $^1\Sigma^-$ – $^1\Pi$ transition.

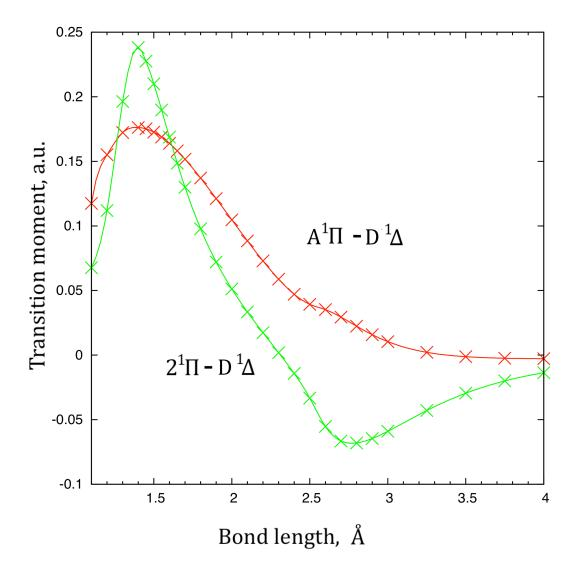


FIG. 5: The computed transition moments for the ${}^{1}\Pi - {}^{1}\Delta$ transition. Note these are the cartesian moment $<\Pi_{x}|y|\Delta_{xy}>$, where $\sqrt{2}<\Pi_{x}|y|\Delta_{xy}>=<\Pi|\frac{(x+iy)}{\sqrt{2}}|\Delta>$